



## Review

## Superoxide dismutases—a review of the metal-associated mechanistic variations

Isabel A. Abreu<sup>a,1</sup>, Diane E. Cabelli<sup>b,\*</sup><sup>a</sup> Plant Genetic Engineering Group, Instituto de Tecnologia Química e Biológica da Universidade Nova de Lisboa, Quinta do Marquês, 2784-505 Oeiras, Portugal<sup>b</sup> Department of Chemistry, Brookhaven National Laboratory, Upton, NY 11973-5000, USA

## ARTICLE INFO

## Article history:

Received 3 September 2009

Received in revised form 4 November 2009

Accepted 5 November 2009

Available online 13 November 2009

## Keywords:

Superoxide Dismutase

Manganese Superoxide Dismutase (MnSOD)

CopperZinc Superoxide Dismutase (CuZnSOD)

Iron Superoxide Dismutase (FeSOD)

Nickel Superoxide Dismutase (NiSOD)

Amyotrophic Lateral Sclerosis (ALS)

Pulse Radiolysis

Stopped Flow technique

## ABSTRACT

Superoxide dismutases are enzymes that function to catalytically convert superoxide radical to oxygen and hydrogen peroxide. These enzymes carry out catalysis at near diffusion controlled rate constants via a general mechanism that involves the sequential reduction and oxidation of the metal center, with the concomitant oxidation and reduction of superoxide radicals. That the catalytically active metal can be copper, iron, manganese or, recently, nickel is one of the fascinating features of this class of enzymes. In this review, we describe these enzymes in terms of the details of their catalytic properties, with an emphasis on the mechanistic differences between the enzymes. The focus here will be concentrated mainly on two of these enzymes, copper, zinc superoxide dismutase and manganese superoxide dismutase, and some relatively subtle variations in the mechanisms by which they function.

Published by Elsevier B.V.

## 1. Introduction

Cellular redox processes such as oxidative phosphorylation may lead to excess electrons in solution. As cells have reasonable oxygen concentrations, superoxide radical ( $O_2^{\cdot-}$ ) can be rapidly formed by attachment of the electron. Superoxide radical is not a particularly strong reductant or oxidant [1], so it is rather unreactive with the amino acids that comprise the protein backbone, with the notable exceptions of the sulfur-containing amino acids, cysteine and methionine. It is, however, very reactive with some transition metal complexes and the corresponding aquated ions, particularly copper, iron and manganese. Additionally, evidence has accumulated for the existence of a number of targets for  $O_2^{\cdot-}$  reactivity *in vivo*. These are mainly soluble proteins containing [Fe-S] clusters, such as aconitase, dehydrases, and fumarases [2,3].

Superoxide dismutases (SODs) are enzymes that function to catalytically convert  $O_2^{\cdot-}$  to oxygen ( $O_2$ ) and hydrogen peroxide ( $H_2O_2$ ) [4–6]. Based on the metal co-factor they harbor, SODs can be classified into four groups: iron SOD (FeSOD), manganese SOD (MnSOD), copper-zinc SOD (CuZnSOD), and nickel SOD (NiSOD). All

four groups can be found in prokaryotic organisms, while in Eukaryotes FeSOD can be found in chloroplasts, MnSOD is the SOD typically found in mitochondria and can also be found in peroxisomes, and CuZnSOD is usually the most abundant SOD and can be found in the chloroplast, in the cytosol and in the extracellular space. These enzymes are thus fairly ubiquitous in aerobic organisms. In addition to SODs, there is a class of enzymes that acts only to reduce  $O_2^{\cdot-}$  to  $H_2O_2$ , hence the name superoxide reductase (SOR). This system can effect the catalytic removal of superoxide only in the presence of an exogenous electron donor to regenerate the original oxidation state of the SOR. It is not discussed here but is reviewed elsewhere in this volume [Pinto et al.]. Recent studies by Culotta, in yeast, show that manganese can serve, independently of its role as MnSOD co-factor, as an important antioxidant backup for CuZnSOD [7]. This work follows important observations showing that high intracellular Mn levels can provide protection against oxidative stress [8,9]. Additional studies have shown that manganese-phosphate complexes can be *in vitro* mimics for SOD [4,10].

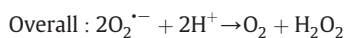
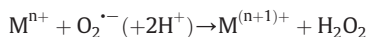
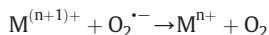
That the catalytically active metal of SODs can be copper, iron, manganese or, recently, nickel is one of the fascinating features of this class of enzymes. In this review, we describe these enzymes in terms of the details of their mechanisms, with an emphasis on the differences that have been characterized between these systems and a special focus on CuZnSOD and MnSOD.

The overall mechanism by which SODs function has been called a “ping-pong” mechanism as it involves the sequential reduction and oxidation of the metal center, with the concomitant oxidation and

\* Corresponding author. Tel.: +1 631 344 4361; fax: +1 631 344 5815.

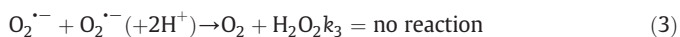
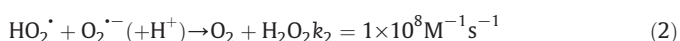
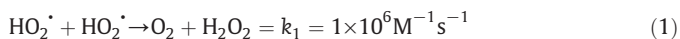
E-mail address: [Cabelli@bnl.gov](mailto:Cabelli@bnl.gov) (D.E. Cabelli).<sup>1</sup> Tel.: +351 214469660; fax: +351 214421161.

reduction of superoxide radicals (Scheme I) at virtually diffusion controlled rates that generally



#### Scheme I

include a pH range (approximately pH 5–9.5) where the rate is unchanging. Superoxide and its conjugate acid, perhydroxyl radical ( $HO_2^{\cdot}$ ), do, however,



undergo spontaneous disproportionation (reactions 1–3) at rates constants dependent upon the protonation state of the oxyradicals and the acid-base equilibrium between the oxy radicals (4, –4) [1]. As seen in Fig. 1, there are two major differences between the metal-mediated catalytic dismutation and the spontaneous disproportionation of total oxy radical ( $O_2^{\cdot-}/HO_2^{\cdot}$ ). The first is that the different rate constants measured for reactions 1–3 [11], particularly the lack of any observable reaction of  $O_2^{\cdot-}$  with itself, lead to a very significant pH dependent spontaneous disproportionation of  $O_2^{\cdot-}/HO_2^{\cdot}$ ; Fig. 1 solid line. The second is that the disproportionation is bimolecular and the half-life for radical disappearance becomes much slower as the concentration of  $O_2^{\cdot-}/HO_2^{\cdot}$  decreases. At pH 7 and micromolar ( $10^{-6}$  M) [ $O_2^{\cdot-}/HO_2^{\cdot}$ ], the half life ( $t_{1/2}$ ) for the dismutation is approximately 10 s. By contrast, the catalytic rate is only dependent upon the concentration of the enzyme. At even nanomolar enzyme ( $10^{-9}$  M), three orders of magnitude less than [ $O_2^{\cdot-}/HO_2^{\cdot}$ ], the  $t_{1/2}$  for enzymatic dismutation is over an order of magnitude faster than that for the spontaneous process; Fig. 1.

As noted earlier, these enzymes are found with a variety of different metal centers and protein structures. Three different protein

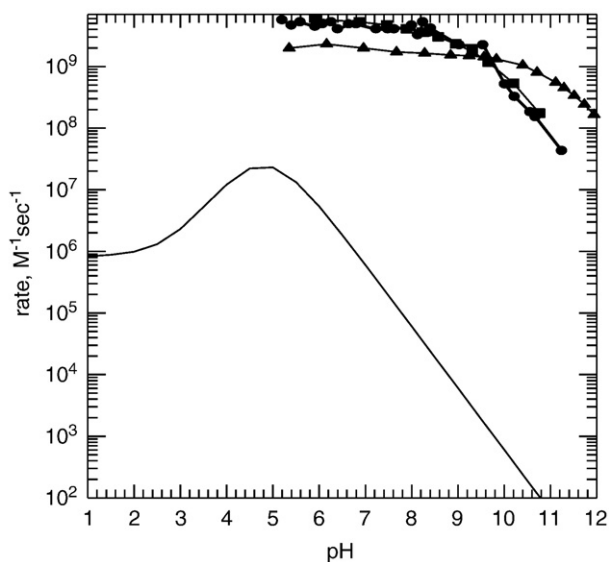


Fig. 1. The pH dependence of the rate constants for disproportionation of  $O_2^{\cdot-}/HO_2^{\cdot}$  (solid black line) and catalytic dismutation of  $O_2^{\cdot-}/HO_2^{\cdot}$  by CuZnSOD (blue triangle), MnSOD (black circle) and NiSOD (red square) on a per enzyme basis.

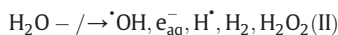
structures have evolved with four different redox active metals, that of CuZnSOD, that of FeSOD/MnSOD and that of NiSOD; see Fig. 2. What is striking is the difference in the protein structures and metal-binding sites in the different enzymes when contrasted to the extraordinary similarity of the enzymatic activity for the different proteins. In this article, we will give a brief discussion of some fast kinetic techniques that allow discrimination of various aspects of the overall mechanism (Scheme I). We will then discuss the enzymes separately by different metal center in order of less mechanistic complexity to greater mechanistic complexity; CuZnSOD, FeSOD, MnSOD and, finally, NiSOD, where much of the mechanistic details are yet to be unraveled. The two enzymes that will undergo the most extensive discussion in this review are CuZnSOD and MnSOD. The readers are referred to other reviews, both in this issue and elsewhere [4–6] for further discussions of various aspects of superoxide dismutases.

## 2. Fast kinetic techniques

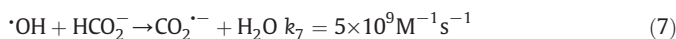
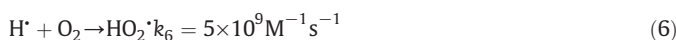
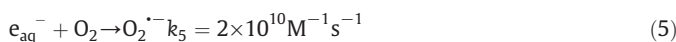
There are two fast kinetic techniques that have proven indispensable to elucidation of the mechanism by which these enzymes function; pulse radiolysis and stopped flow techniques.

### 2.1. Pulse radiolysis

Pulse radiolysis involves the rapid, sub-microsecond, pulsed deposition of energy, in the form of accelerated electrons, into a solution [12,13]. Here we will discuss pulse radiolysis in water only as that is the medium of these enzymes. Upon radiolysis of water, the following species are produced, where the values in brackets are G values, the yield per 100 eV energy deposited. In the presence of oxygen



and formate or ethanol, the primary radicals are converted to  $O_2^{\cdot-}/HO_2^{\cdot}$  (reactions 5–9 and equilibrium 4) at well-established very rapid rates [14]. This allows rapid generation of the substrate for SOD catalysis in water containing no more than millimolar concentrations of the aforementioned scavengers.



The most convenient detection method for pulse radiolysis studies involves monitoring changes in the ultraviolet/visible (UV/Vis) absorbance (200–800 nm) of transient species. Taking advantage of the known absorbances [1] of  $O_2^{\cdot-}/HO_2^{\cdot}$ ; Fig. 3, the change in absorbance with time at 220–290 nm is measured to obtain kinetic data. The major advantages of this technique are (i) the extremely “clean” method of  $O_2^{\cdot-}$  production, requiring only water, oxygen and formate and (ii) the extremely rapid, sub-microsecond, generation of  $O_2^{\cdot-}$  that allows a large time window for measuring reaction kinetics. These features have made pulse radiolysis a major tool in establishing the details of the enzymatic mechanisms for all of the SODs. The major

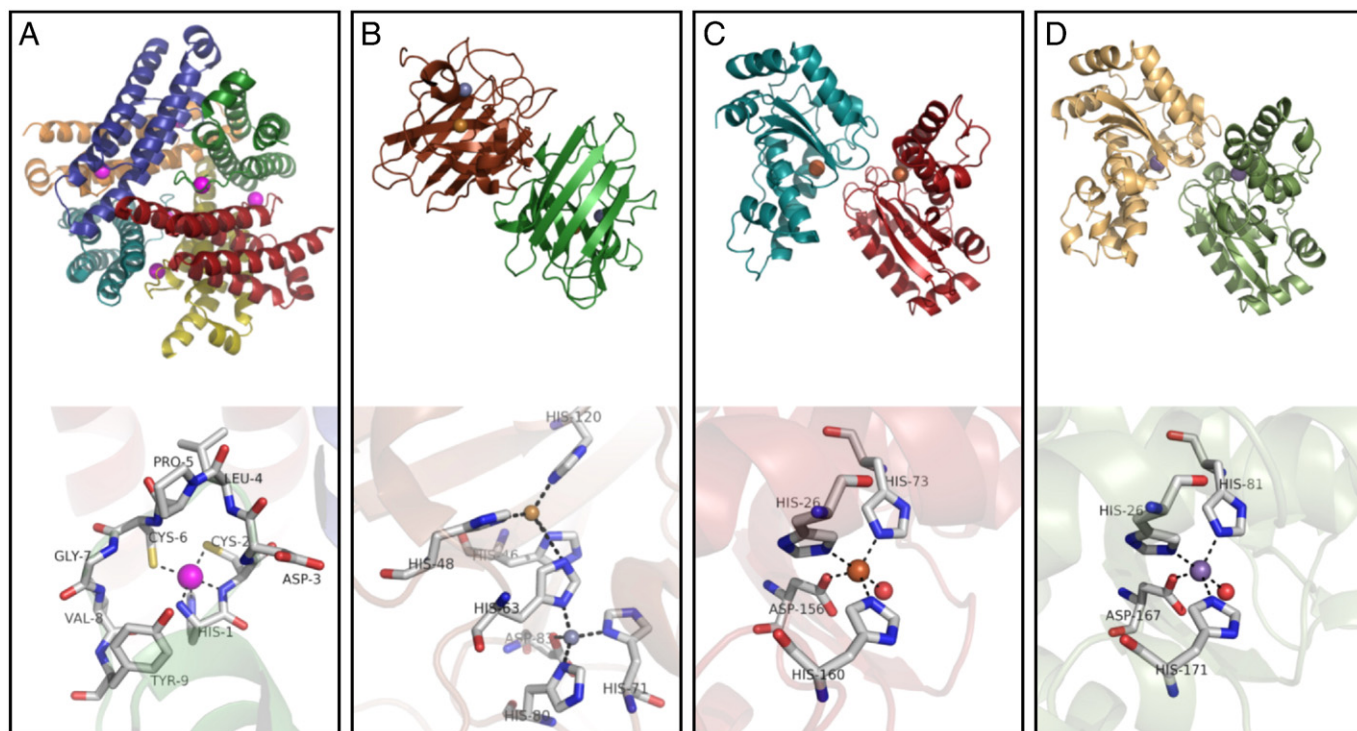


**Fig. 2.** A comparison of the enzyme structures and active sites for the four SODs, (A) *Streptomyces coelicolor* NiSOD (pdb ref.: 1t6u [90]), (B) human CuZnSOD (pdb ref.: 1pu0[94]), (C) *E. coli* FeSOD (pdb ref.: 1isa [18]) and (D) MnSOD (pdb ref.: 1vew [95]). Picture created with PyMOL [96].

limitations with this technique are (i) the concentration of  $O_2^{\bullet-}/HO_2^{\bullet}$  generated in a pulse of electrons realistically is between 0.5 and 50 micromoles and (ii) the requirements for an accelerator that removes it from a routine laboratory capability. It is these limitations that led to the very effective use of stopped flow techniques.

## 2.2. Stopped flow technique

In contrast to pulse radiolysis, the stopped flow technique involves the rapid mixing of solutions, in this case one contains  $O_2^{\bullet-}$  and the other contains the SOD of interest. Again, detection involves UV/Vis absorption but here the time resolution is limited by the mixing time,

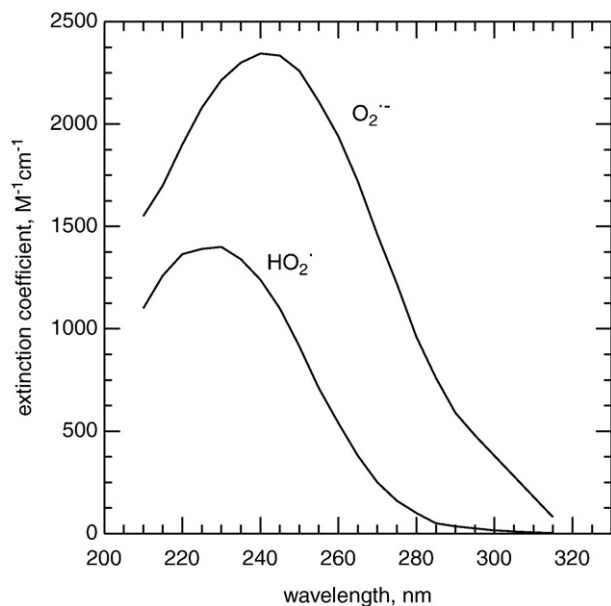


**Fig. 3.** The spectra of  $O_2^{\bullet-}/HO_2^{\bullet}$ .

generally approximately 1 ms. It is the inability to monitor reactions on the sub-millisecond timescale that is the most significant limitation in using stopped-flow techniques. The advantage here, in addition to the general availability of the instrumentation, is that  $[O_2^{\bullet-}]$  is limited only by the concentration that is stable in solution. Realistically, millimolar superoxide is the upper concentration limit as dismutation of  $O_2^{\bullet-}$  produces  $O_2$ , which is only soluble to approximately 1.2 mM in water at ambient temperature, neutral pH and 10 mM salt. Therefore, much more than 2 mM  $O_2^{\bullet-}$  (1 mM  $O_2$ ) will lead to a supersaturated solution and  $O_2$  bubbles, which will perturb measurement of reaction kinetics. Stopped flow studies are only possible because of the stability of salts of superoxide, such as  $KO_2$  or tert-butylammonium superoxide [15] in dimethylsulfoxide (DMSO) or the stability of  $O_2^{\bullet-}$  at high pH in water. In the former scenario, stable solutions of  $DMSO-O_2^{\bullet-}$  can then be mixed in a 1:10 ratio (either with a single mixer or a triple mixer system) with water containing the enzyme. In the latter scenario, relatively stable high pH solutions of  $O_2^{\bullet-}$  can be prepared as, at pH 12 for example, the half-life for spontaneous disappearance of 1 mM  $O_2^{\bullet-}$  is 230 s. The only caveat here is that the pH dependent and concentration dependent disproportionation of  $O_2^{\bullet-}$  must be considered for the concentrations used here, which are generally in the 0.05–1 mM range. That necessitates that most studies are carried out at greater than neutral pH because, at pH 7, 1 mM  $O_2^{\bullet-}$  has a half-life of ca 2 ms, almost the time resolution of the instrument. This technique, developed by Fee and co-workers [16–18], was used to great advantage to address primarily substrate inhibition, as will be discussed later.

## 3. Copper, zinc superoxide dismutase

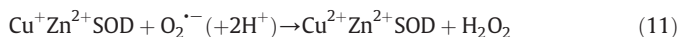
In a 1969 landmark study, McCord and Fridovich [19] demonstrated that a well-known blue copper protein, erythrocyte, carried out the rapid catalytic dismutation of superoxide and renamed this protein superoxide dismutase. CuZnSOD is a dimeric enzyme with each monomeric unit containing an active site of one copper and one zinc bridged by a histidine imidazole. The copper is bound by 3 additional histidines with an overall distorted square planar structure

and an additional water molecule. The zinc is bound by two histidines and an aspartate in addition to the bridging imidazole. Copper is the redox-active metal, changing between the 2+/3+ oxidation states during catalysis, and zinc appears to play a role in overall enzyme stability and in facilitating a large pH independence in activity. Upon reduction of the  $\text{Cu}^{2+}\text{Zn}^{2+}\text{SOD}$  to  $\text{Cu}^+\text{Zn}^{2+}\text{SOD}$ , the bridging imidazole-copper coordination is lost, as is the bound water and the  $\text{Cu}^+$  shifts position and is three coordinate; otherwise both oxidized and reduced enzymes are generally structurally similar [20].

A pathway for copper insertion into the CuZnSOD protein has been shown to occur in yeast through a copper chaperone for superoxide dismutases; namely CCS [21]. This chaperone has three distinct protein regimes, known as Domain I, Domain II and Domain III, with the largest, Domain III, resembling the monomeric unit of CuZnSOD. Studies have shown that domain I is responsible for acquiring the copper and transferring it to domain III. Domain III is then able to insert the copper into the apo SOD that has colocalized with the monomeric SOD. Interestingly, this part of CCS (Domain II) has what resembles the copper-binding site in SOD but is missing one of the binding histidines and has been shown to be unable to bind copper itself [22]. A review of this process is given in Culotta et al. [21, 23] and fascinating studies of the role of copper and CCS regulation was carried out by the Gitlin group [24].

### 3.1. The dismutase mechanism

The first studies using pulse radiolysis showed that catalysis was virtually diffusion controlled and pH independent (pH 5–9.5);  $k_{\text{cat}} = k_{10} = k_{11} \approx 2 \times 10^9 \text{ M}^{-1} \text{ s}^{-1}$  [25,26]. Studies at very high



concentrations of  $\text{O}_2^{\cdot-}$  [11], carried out as described in Section 2.2, show that if a saturative mechanism is operative, it must occur with a  $K_m$  that is greater than 5 mM  $\text{O}_2^{\cdot-}$ . Subsequently, it was suggested that the relatively slow “diffusion controlled” rate constant of  $2 \times 10^9 \text{ M}^{-1} \text{ s}^{-1}$  was actually unexpectedly high because, given the surface area differential between  $\text{O}_2^{\cdot-}$  and CuZnSOD (approximately 1:150), the actual measured rate constant should have been an order of magnitude slower for a diffusion-controlled process [27,28]. The measured rate constants were suggested to result from the electrostatic guidance of the negatively charged  $\text{O}_2^{\cdot-}$  into the positively charged active site. This suggestion was corroborated by enzymatic and theoretical studies [28,29]. Detailed pulse radiolysis studies as a function of both ionic strength and pH of the activity of various mutations of the positively charged arginine at the entrance to the active site channel showed that the positive charge on the arginine was responsible for much of the electrostatic guidance [30]; Fig. 4. The net effect of changing the charge on that arginine is an order of magnitude drop upon neutralization of the positive charge and another order of magnitude drop upon reversing the charge. This is corroborated by the observed change in rate constant with pH; upon protonation of the anionic oxygen in the glutamate/aspartate, the order of magnitude decrease in the rate constant is regained. An additional study showed that neutralizing the negatively charged glutamate near the active site led to a faster enzyme [31] than the wild-type enzyme, again corroborating the electrostatic guidance of superoxide to the active site.

As stated above, zinc in the active site facilitates pH independence to catalysis although it is not redox active. One of the unique capabilities that results from the time resolution afforded by pulse radiolysis is the ability to look at the individual reactions of the overall catalytic mechanism. This is accomplished by using conditions where the

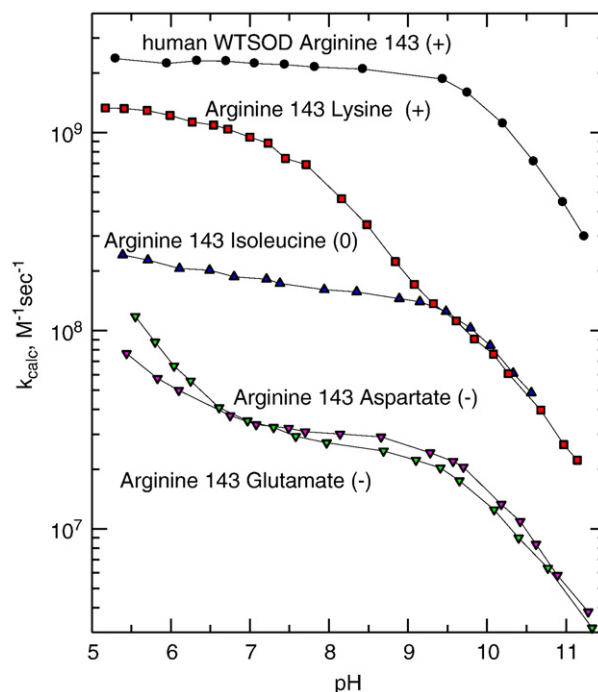


Fig. 4. Rate constants for  $\text{O}_2^{\cdot-}$  dismutation by wild-type and various Arginine 143 mutants of human sCuZnSOD as a function of pH (20 mM phosphate, 10 mM formate, 5  $\mu\text{M}$  EDTA). The charge on the new residue is indicated in brackets.

enzyme is at a high concentration relative to  $\text{O}_2^{\cdot-}$  so that only the  $\text{O}_2^{\cdot-}$  oxidation (reaction 10) or the  $\text{O}_2^{\cdot-}$  reduction (reaction 11) half of the system occurs. Given the magnitude of the absorbance associated with the protein at 240–290 nm, where  $\text{O}_2^{\cdot-}$  absorbs, this experiment is carried out by following the disappearance or regrowth of the copper (II) absorbance at 680 nm. Using this technique, it was shown much earlier that in the fully metallated enzyme both reactions 10 and 11 individually occur at  $2 \times 10^9 \text{ M}^{-1} \text{ s}^{-1}$  [25,26]. However, studies showed that the rate constant for  $\text{O}_2^{\cdot-}$  dismutation by CuapoSOD, that is the enzyme with copper in both copper sites of the dimer but no zinc in the zinc sites, begins to slow at pH ca 7 [32], and references therein]. A careful study of the dismutation of  $\text{O}_2^{\cdot-}$  by CuapoSOD as a function of pH allowed an exploration of the difference between reaction 11 and the overall catalytic mechanism. An examination of the kinetics of reduction of  $\text{Cu}^{2+}$ apoSOD by  $\text{O}_2^{\cdot-}$  (reaction 10) demonstrated that enzymatic reduction and concomitant superoxide oxidation was pH independent. However, the rate of  $\text{Cu}^+$ apoSOD oxidation, with concomitant  $\text{O}_2^{\cdot-}$  reduction to peroxide (reaction 11) was shown to be pH dependent, leading to the overall pH dependence of catalysis described above. The overall conclusion was that the zinc-bridging imidazole moiety plays a crucial role in the pH independence observed in the CuZnSOD dismutation mechanism by maintaining the geometry of the copper coordination sphere that allows the rapid dissociation of the bound peroxide [32].

### 3.2. The peroxidase mechanism

The other catalytic cycle in CuZnSOD is a peroxidative cycle that is described by reactions 11 and 12, the reactions of peroxide with both the reduced and oxidized enzyme [33,34].



The significance of this cycle is that reaction 13 is a Fenton-type reaction, where the reduced metal can actually serve to cleave the O-O

bond in H<sub>2</sub>O<sub>2</sub> into the OH radical and the hydroxide ion (OH<sup>-</sup>). When the dismutase and peroxidase cycles are combined (reactions 10–13), removal of O<sub>2</sub><sup>-•</sup> leads to catalytic generation of both O<sub>2</sub> and OH<sup>-</sup> and regeneration of 1/4 of the H<sub>2</sub>O<sub>2</sub>. Studies have demonstrated that the OH radical does not freely diffuse from the active site but that it is bound and can therefore attack the copper-binding histidines at the active site [34], leading to copper loss and deactivation of the CuZnSOD. It can also undergo scavenging by an external substrate that can get near enough to the active site [34]. More recently, studies involving peroxide addition to the enzyme followed by time-of-flight mass spectrometry have shown which copper-binding histidines are subject to oxidative damage by the bound OH radical [35] and, as suggested earlier, the copper and zinc bridging His61 was the predominant site of OH radical attack. In reaction 13, the hydroperoxyl anion was written as the reactive species, as reflected by the hydrogen peroxide/hydroperoxyl anion equilibrium (14, –14). This was shown in two studies [36,37] where the pH dependence of inactivation showed clearly that between pH 7 and 10, *k*<sub>13</sub> increased an order of magnitude for each pH unit increase



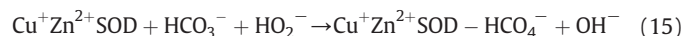
The peroxidative cycle (reactions 12 and 13) describes a method for conversion of the more unreactive O<sub>2</sub><sup>-•</sup> radical into the much more reactive OH radical, albeit at a very slow rate at neutral pH. This pathway gained increasing importance with the relatively recent connection between Lou Gehrig's disease and mutant forms of CuSODs [38,39], discussed below.

### 3.3. Familial amyotrophic lateral sclerosis and CuZnSOD

Almost two decades ago, studies began linking approximately 20% of inherited or familial version of amyotrophic lateral sclerosis (fALS, Lou Gehrig's disease) to damage to the gene on chromosome 21 that is responsible for the expression of Cu,ZnSOD [40]. This linkage was confirmed when transgenic mouse models were produced expressing the human CuZnSOD with fALS associated point mutations to the protein (Glycine93Alanine, Glycine37Arginine and Glycine86Arginine) and these mice exhibited the symptoms of ALS [41–43]. To date, fALS has been associated with a large number (over 100) point mutations, deletions and truncations in the protein amino acid residues in human CuZnSOD. Initially, this association was thought to involve an upregulation or a downregulation of enzyme expression or activity. However, it was rapidly demonstrated that in fact it was a new function of the enzyme that was the causative factor in fALS [44]. Careful pulse radiolysis studies of the activities of large number of the isolated mutant enzymes have demonstrated wild-type like activity for all but a subset of mutations that involve copper binding ligands or residues that affect the copper binding ligands [45].

One postulate for the gain-of-function was thought to involve the upregulation of the peroxidase-like mechanism as described in reactions 12 and 13 [46,47]. The gain-of-function could involve either loss of the evolved OH radical into solution, leading to oxidative damage or capture of the OH radical by a binding histidines and release of free copper in the solution with concomitant formation of apo enzyme. Studies of a fALS mutant enzyme (G93A) demonstrated that the peroxidative activity was not increased and that an increase in peroxidative activity was observed instead for CuCuSOD as versus CuZnSOD, regardless of mutation [48]. Subsequent studies showed that the fALS mutant enzymes did, however, mis-metallate in vitro, potentially leading to a CuCuSOD [49]. However, as isolated fALS mutant enzymes appear to be properly metallated so this should be taken as an indicator of a metal-binding site that is perturbed from the wild-type CuZnSOD, although the actual mutation is often far from the metal binding site or even in the second sphere of coordination.

In the course of exploring the fALS connection, some very interesting mechanistic studies were carried out addressing the peroxidase cycle of CuZnSOD. In particular, the influence of bicarbonate (HCO<sub>3</sub><sup>-</sup>), a molecule found in 20–50 mM concentration in human cells, on the peroxidative cycle was explored. As discussed above, the OH radical can be scavenged by an external substrate. However, in the presence of bicarbonate, a conundrum seemed to occur. Here, bicarbonate seemed to be a prooxidant, leading to excessive oxidative damage to a substrate [50] and, at the same time, did not protect the enzyme from oxidative damage [51]. That led to a proposal that carbonate and peroxide, in the presence of the reduced copper, form a peroxomonocarbonate species, as illustrated in reaction 15 [52,53]. It was later shown that the reaction likely occurs through the reaction



of carbon dioxide (CO<sub>2</sub>) and not HCO<sub>3</sub><sup>-</sup>, which are in a well-established where the pK between carbon dioxide and



bicarbonate anion is 6.1 at the in vivo temperature of 37°C. The intermediacy of peroxy-monocarbonate has been demonstrated in a recent NMR and EPR study [54].

The current thinking on the gain-of-function of the fALS mutant protein does not involve a mechanism of oxidative damage to substrates but rather seems to implicate the different aggregation propensities of the mutant apo-protein. The involvement of the actual dismutase/peroxide mechanism might lie in the question of whether oxidative damage of the protein and subsequent metal loss is playing a role or whether there are actually a number of different mechanisms associated with the mutant enzyme-induced disease. The reader is referred to review articles cited here as an involved discussion is beyond the scope of this article [48,55].

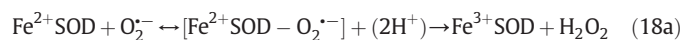
## 4. Iron superoxide dismutase (FeSOD)

Iron superoxide dismutase (FeSOD) is a prokaryotic enzyme found primarily in the cytosol of plant and some bacterial cells. It has a protein structure that is akin to that of manganese superoxide dismutase (MnSOD) and therefore clearly co-evolved. The two enzymes have, however, maintained their metal selectivity; that is a manganese ion introduced into the active site of FeSOD leads to very slow dismutases activity and vice versa. There is a small group of enzymes called cambialistic enzymes because they will actually function with either metal although the overall dismutation rate does not appear to be optimized to that measured in the metal-specific analogues. FeSODs are dimers with each iron active site containing a single iron bonded to three histidines, one aspartate and one water [18].

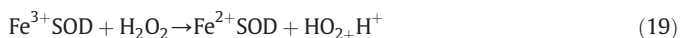
The overall superoxide dismutase mechanism is, again, the ping-pong mechanism as seen in reactions 17 and 18 [56]. However, stopped-flow studies, where the O<sub>2</sub><sup>-•</sup> concentration can be very



high [57], indicate that *K<sub>m</sub>* here is approximately 100 μM, suggesting that reaction 18 needs to be modified to include the saturative process and the mechanism is actually described by reaction 17 followed by reaction 18a. However, saturation is not observed with all FeSODs [58].



The FeSOD also has a parallel peroxidative mechanism where again, reduction of  $\text{Fe}^{3+}$ SOD by  $\text{H}_2\text{O}_2$  (reaction 19) is faster than the corresponding reaction of  $\text{H}_2\text{O}_2$  with  $\text{Fe}^{2+}$ SOD (reaction 20) [59].



This is not surprising as it was the reaction of free iron with hydrogen peroxide that led to the observation of the Fenton reaction. The great interest in FeSODs has involved redox tuning and the geometry and dynamics of inhibition with various anions such as azide. These topics are reviewed extensively in this volume.

## 5. Manganese superoxide dismutase

MnSODs are manganese containing enzymes first discovered by Fridovich and co-workers [60]. These enzymes are well conserved throughout evolution and across Kingdoms. As mentioned before, they share a very high sequence and protein fold homology with FeSODs. MnSODs are found as dimers or tetramers, with a single manganese atom per subunit. Dimeric forms of MnSOD are typically found in bacteria, while Eukaryotes usually harbor tetrameric MnSOD. The active site is invariant, with the manganese bound in a trigonal bipyramidal geometry to four ligands from the protein (three histidine and an aspartic acid residue) and a fifth solvent ligand.

This latter ligand is postulated to be a hydroxide when manganese is in its oxidized form and to protonate upon manganese reduction; see Fig. 5 for the overall protein and active site structures for three different MnSODs. The manganese is recessed in the active site cavity with a hydrogen-bonded network that extends from the bound water and comprises the side chains of several residues, most significantly a tyrosine and a glutamine (Y34 and Q143, respectively, in human MnSOD), and finally an adjacent water molecule that sits at the opening of the cavity. The role of this hydrogen bonded network is presumably to facilitate proton transfer upon reduction of  $\text{O}_2^{\cdot-}$  to  $\text{H}_2\text{O}_2$ .

Due to high sequence and structure homology to FeSOD, with virtually superimposable metal binding sites, MnSOD can incorporate iron instead of manganese in the active center; *Escherichia coli* MnSOD has been shown to incorporate iron *in vivo* in anaerobic conditions and/or with high extracellular Fe concentrations present. When iron replaces manganese in the active site of *E. coli* MnSOD, the enzyme becomes inactive. Although it can still reduce  $\text{O}_2^{\cdot-}$ , it no longer oxidizes  $\text{O}_2^{\cdot-}$  due to its reduction potential of  $-240$  mV (vs. NHE), which is lower than the reduction potential for the pair  $\text{O}_2/\text{O}_2^{\cdot-}$  [61]. It appears that the reduction potential for the iron in the SOD active site is strongly influenced by some residues in the metal second-sphere of coordination. In particular, it is affected by the glutamine that sits in the hydrogen-bonded network (Q143 in human MnSOD) and that also seem to affect metal ion binding affinities (see [62] for an extended review of this subject).

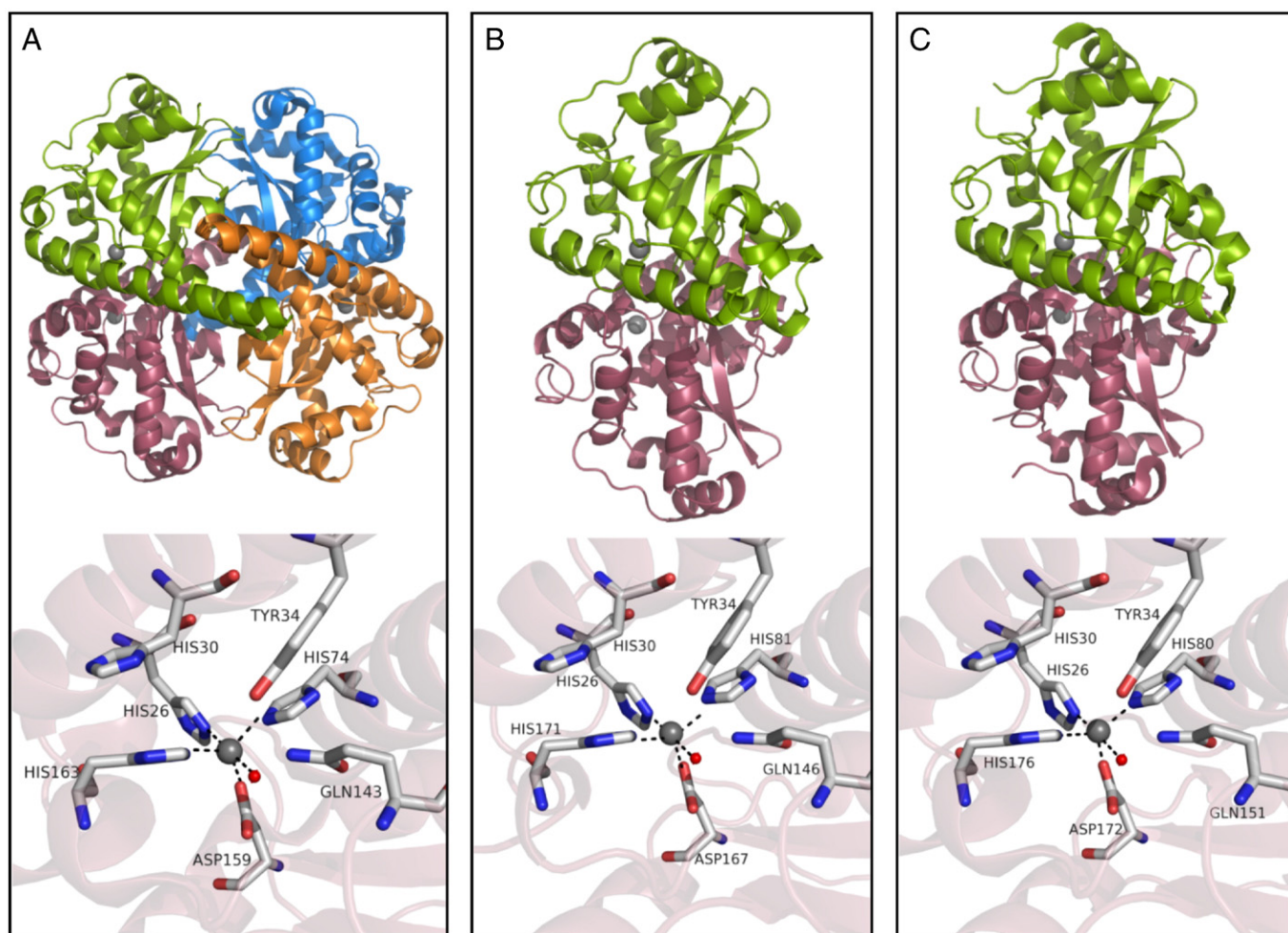


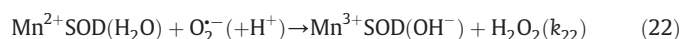
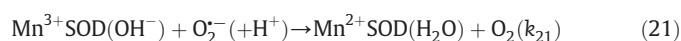
Fig. 5. Comparison of quaternary structures and active sites of (A) human (pdb ref.: 1n0j [97]), (B) *E. coli* (pdb ref.: 1vew [95]) and (C) *D. radiodurans* (pdb ref.: 2ce4 [98]) MnSOD. Picture created with PyMOL [96].

In bacteria, MnSOD is cytosolic, while in eukaryotes it is usually found in the mitochondrial matrix. Eukaryotic MnSOD is encoded by a nuclear gene and its polypeptide has to be imported into the mitochondria through the identification of an N-terminal mitochondrial signal peptide that is cleaved upon mitochondrial import. Several studies by Culotta et al. in *Saccharomyces cerevisiae* MnSOD, show that the absence of the mitochondrial signal peptide results in protein accumulation in the yeast's cytosol. This protein is inactive due to lack of manganese, demonstrating that yeast MnSOD requires mitochondrial localization in order to be properly loaded with Mn [63]. Proper manganese loading into yeast MnSOD is also dependent on the presence of both Smf2p, a Nramp Mn ion transporter in yeast, essential to the delivery of Mn to the mitochondrial matrix [64], and Mtm1p, a member of the mitochondrial carrier family (MCF) of transporters [65]. Mtm1p is essential for Mn-binding by yeast MnSOD in mitochondria [65], but it is not clear if it acts as a chaperone for Mn-loading. The identification of an Mtm1p homologue in the plant model *A. thaliana* that can complement yeast *mtm1* mutants [66] and of a human homologue *MTM1*, CGI-69 gene [65], suggests that the Mtm1p function in eukaryotic MnSOD assembly may be as ubiquitous as mitochondrial MnSOD itself.

The *in vitro* metallation of *E. coli* MnSOD has been the subject of many elegant studies from the Whittaker lab [67,68]. The mechanism has been demonstrated to be complex and reflect a thermally controlled process to allow a form in which the apo enzyme can bind manganese and then a conformational change to a final, stable metal bound enzyme. Interestingly, the apo enzyme maintains its dimeric structure and, upon introduction of the metal, a conformational change involving a proton transfer with a pK of 7.7 leads to the stable metallated enzyme. It was the observed zero-order kinetics of the metal-loading processes led the authors to introduce the idea of a conformational change. This is a similar concept to the “gating” that is described below in the dismutase mechanism, although on a very different time scale; the metal-loading process takes many minutes while the “gating” in the dismutases cycle is on the millisecond time scale.

### 5.1. The dismutase mechanism

Like other SODs, the MnSOD dismutation mechanism involves cycling between oxidized ( $\text{Mn}^{3+}$ ) and reduced ( $\text{Mn}^{2+}$ ) metal. The significant difference in the mechanism of MnSOD with that of other SODs is that the simple first-order disappearance of  $\text{O}_2^{\cdot-}$  is not observed at sufficiently high ratios of  $[\text{O}_2^{\cdot-}]:[\text{MnSOD}]$ , instead, there is a “burst phase” and a “zero-order” phase. This led to a mechanism where, in its reduced form, MnSOD has been suggested to react with superoxide through two concomitant pathways [17,69,70]. Thus the overall proposed mechanism (reactions 21 to 24) includes the formation of  $\text{Mn}^{3+}\text{SOD}-\text{O}_2^{2-}$ , formed in parallel with  $\text{Mn}^{3+}\text{SOD}$ , often called the inhibited complex.



A more complex scheme to explain MnSOD catalytic mechanism which allows for reversibility of steps was proposed by Bull et al. [17]. Here the inhibited complex is rather viewed as a reversible, dead-end complex, and is formed from an enzyme substrate complex rather than directly from superoxide reaction with  $\text{Mn}^{2+}$ . The simpler mechanism described in reactions 21–24 is just a special case of the full Bull et al treatment and was suggested initially from pulse

radiolysis studies of the dismutases mechanism by following the disappearance of a relatively high concentration of  $\text{O}_2^{\cdot-}$  in the presence of a catalytic concentration of MnSOD [61,62]. Another way to confirm this mechanism is to measure the growth of the absorption of  $\text{Mn}^{3+}\text{SOD}$  in the visible region (350–600 nm) upon rapid generation of substoichiometric amounts of  $\text{O}_2^{\cdot-}$ . In the presence of a high concentration of the reduced  $\text{Mn}^{2+}\text{SOD}$ ; see Fig. 6. Here, as expected, in the presence of *E. coli* MnSOD, reaction 2 occurs and the absorbance corresponding to  $\text{Mn}^{3+}\text{SOD}$  grows in with a rate constant of  $2 \times 10^9 \text{ M}^{-1} \text{ s}^{-1}$  per dimer. However, when human  $\text{Mn}^{2+}\text{SOD}$  reacts with substoichiometric  $\text{O}_2^{\cdot-}$ , there is an initial growth followed by a slower process that leads to stoichiometric formation of  $\text{Mn}^{3+}\text{SOD}$ . The absorbance that grows in with the rate constant of  $4 \times 10^9 \text{ M}^{-1} \text{ s}^{-1}$  (per tetramer) corresponds to that of both  $\text{Mn}^{3+}\text{SOD}(\text{H}_2\text{O})-\text{O}_2^{2-}$  and  $\text{Mn}^{3+}\text{SOD}$  with the slower process representing reaction 24.

In the following sections we will first discuss the catalytic mechanism, mainly in terms of reaction 21. Then we describe the “inhibited complex” and the implications in terms of high or low  $\text{O}_2^{\cdot-}$  concentration. This then leads to a discussion of the variation in the rate constants for reactions 21–24, and more specifically, reactions 22 and 23, between species.

#### 5.1.1. Catalysis

There has been a great deal of study of the protonation process in the catalytic mechanism as a result of the 2 proton requirement to go from  $\text{O}_2^{\cdot-}$  to  $\text{H}_2\text{O}_2$ . Reaction 21 shows a bound hydroxide to the MnSOD that is protonated to bound water as a part of the reduction process. That this occurs was shown in some very elegant experimental studies by Miller et al [71] and is a way to account for the first proton that is required to protonate off the bound peroxy moiety. Tyrosine 34 is in the second sphere of coordination of the Mn and part of the hydrogen-bond network that is involved in proton transfer during catalysis. DFT calculations show that Y34 is essential to maintain a bound hydroxide (as versus water) to  $\text{Mn}^{3+}$ , because it puts a thermodynamic barrier for proton transfer that is only lowered upon superoxide binding, facilitating proton transfer as part of metal- $\text{O}_2^{\cdot-}$  electron transfer [72]. Any change in Y34 raises this barrier to proton transfer, making  $\text{O}_2^{\cdot-}$  binding an exclusive pathway for proton transfer to the bound hydroxide [72] and is expected to have an effect on reaction (21). The substitution of Y34 in the human enzyme leads to virtual shut-down of catalysis through reactions 21 and 22. This can

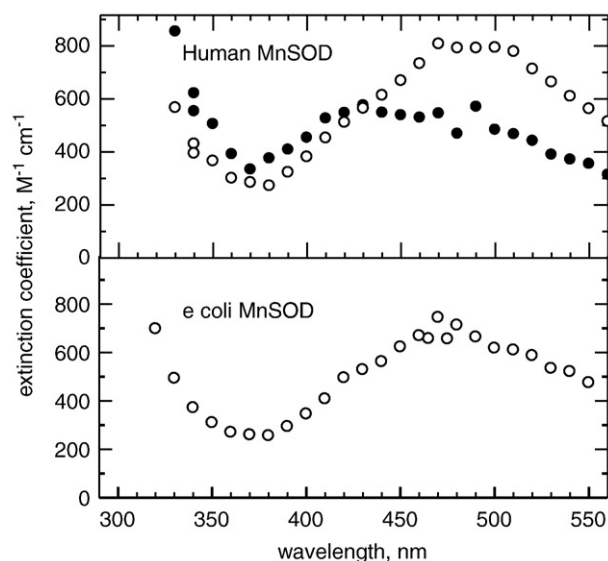


Fig. 6. Spectra of  $\text{Mn}^{3+}\text{SODs}$  (open circles) and  $\text{Mn}^{3+}\text{SOD}(\text{H}_2\text{O})-\text{O}_2^{2-}$  (closed circles) as measured in pulse radiolysis experiments.

be observed for Y34A [73], and Y34F [74] where  $k_{22}$  (reaction 22) becomes insignificant ( $<0.02 \text{ nM}^{-1} \text{ s}^{-1}$ ) when compared to  $k_{21}$  and  $k_{23}$ . In human Y34 mutants, reduction of superoxide happens almost exclusively through inhibited-product formation, most probably due to an important role of Y34 in the proton transfer in reaction 22 as the Y34F redox potential is not changed when compared to WT protein [75]. Significant decreases can also be observed in  $k_{21}$  and  $k_{23}$ , but only to a minor extent relative to that observed for  $k_{22}$ . Nitration of Y34, in human MnSOD, inhibits catalysis [76]. The authors propose this to be due to steric impediment, hydrogen-bond network disruption, and/or possible alteration of the redox potential, although no redox potential measurements were done.

Both in *Deinococcus radiodurans* and *E. coli*, Y34F substitutions do not have such severe effects on  $k_{22}$ . In *D. radiodurans* MnSOD,  $k_{21}$  and  $k_{22}$  decrease  $\sim 25\%$  and  $\sim 20\%$ , respectively, while  $k_{23}$  increases ca. 15% [77]. This renders the enzyme a more human-like catalysis, since  $k_{22}/k_{23}$  becomes close to 1. *E. coli* Y34F decreases catalysis by  $\sim 20\%$ , while Y34A remains WT-like [78]. The caveat here is the conditions under which catalysis is measured for the *E. coli* mutants. If experimental conditions are such that  $k_{24}$  has a half-life that is substantively shorter than the half-life of the initial concentration dependent catalysis, then the saturative process is not significant. This is seen where the concentration of the enzyme is in the nanomolar range because the generation of  $\text{O}_2^{\cdot -}$  is in the sub-micromolar per second range.

The maintenance of the hydrogen-bonded network seems to be crucial to reach WT levels of catalysis in human MnSOD. Glutamine 143 forms a hydrogen-bond with the manganese-bound water and with the hydroxyl side chain of Y34. Replacement of Q143 by alanine or asparagine introduces two or one water molecule in the active site

cavity that complete the hydrogen-bonded network [79,80] (Fig. 7). Nevertheless, Q143A and Q143N are unable to maintain stability and catalytic activity of WT human MnSOD. Mutations on Q143 have been shown to change metal specificity and active site redox potential while also contributing to the decrease in catalysis for these mutants [62,79]. In contrast, mutations of histidine 30 that sits in the opening of the active-center cavity and that was also proposed to be part of the hydrogen-bond network proved to induce no change in the redox potential of the metal active site [81]. The H30V mutation shows highly decreased catalysis and very high product-inhibition, probably due to the steric impediment for  $\text{O}_2^{\cdot -}$  binding introduced by the valine [81], while H30N promotes a higher protonation off of the product inhibited complex, although inducing a small decrease in catalysis [82].

Other single point mutations were made in order to try to understand catalysis in human MnSOD. Tryptophan 161 forms the hydrophobic side, opposite to the cavity opening, of the enzyme's active site. Changes in W161 induced structural changes in adjacent residues, in the hydrogen-bonded network, such as Y34 and Q143, and in the case of W161A introduce a water molecule close to the active site, thus changing the redox potential [83]. W161A and W161F mutations decreased catalytic activity by a factor of 20 and a factor of 4 respectively, when compared to WT. Another example is the glutamic acid 162 that spans the dimeric interface of the tetramer and forms a hydrogen bond with histidine 163 of a neighboring subunit; His 163 is a ligand to Mn. Both E162A and E162D mutations resulted in approximately a factor of 4 to 8 decrease in  $k_{21}$  and  $k_{22}$  respectively, resulting in diminished level of catalysis [84].

Overall, point mutations in human MnSOD tend to highly affect catalysis when the mutated residues are those necessary for

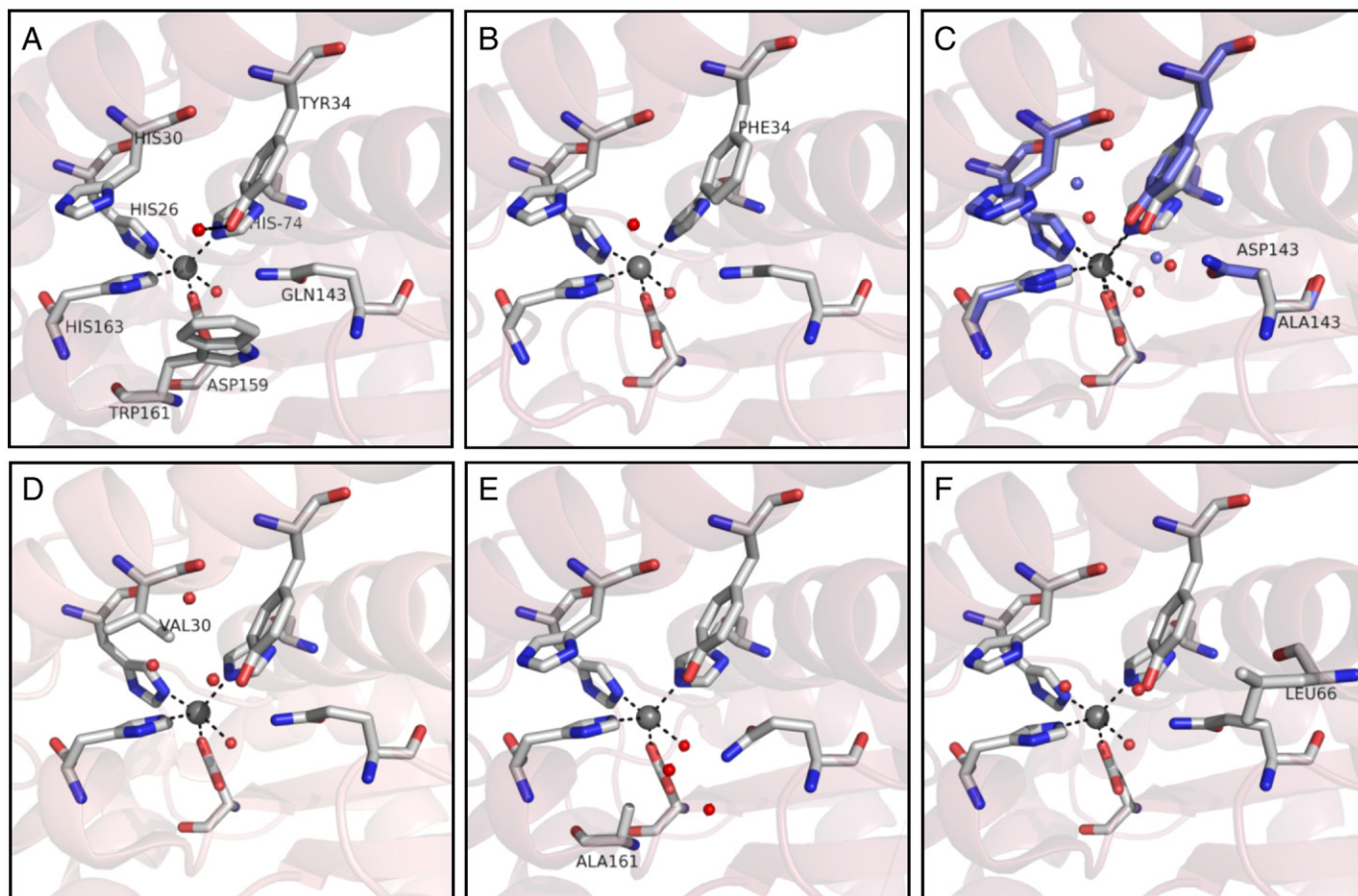


**Fig. 7.** Structural effects of single mutations on the active center of human MnSOD. (A) WT (pdb ref.: 1n0j [97]); (B) Y34F mutation (pdb ref.: 1ap5 [99]); (C) Q143A—white carbon atoms and Q143N—blue carbon atoms (Q143A-pdb ref.: 1em1 [79]; Q143N-pdb ref.: 1qnm [80]); (D) H30V mutation (pdb ref.: 1n0n); (E) W161A (pdb ref.: 1ja8 [83]); (F) F66L mutation (pdb ref.: 2qkc [85]). Picture created with PyMOL [96].

maintaining the hydrogen-bonded network in the active site. In this case,  $k_{22}$  (reaction 22) is strongly affected and catalysis is now significantly dependent upon the inhibited-product dissociation rates ( $k_{24}$ ). Other point mutations can affect the different rate constants in the mechanism, but usually leave the gating unaltered ( $k_{22}/k_{23} = 1$ ). An exception is the mutation F66L [85]. With a  $k_{22}/k_{23} \sim 4$ , due essentially to a significant decrease of  $k_{23}$ , the protein shows less product inhibition and consequently a more *E. coli*-like catalysis, where  $k_{22}/k_{23} \sim 5$ ; Table 1.

### 5.1.2. Product inhibition

The true nature of the inhibited complex is not yet known, but spectroscopic and computational studies [17,86] support the formation of a side-on peroxy complex of the metal. The actual physical process has been suggested to be an isomerization between a side-on and end-on bound peroxy moiety [17]. Our own density-functional theory (DFT) calculations show that side-on conformations, when  $O_2^{\cdot-}$  binds to  $Mn^{2+}$ -SOD, are not stable and spontaneously transform into end-on conformations [72]. As noted above, we could also show that cooperativity exist between  $O_2^{\cdot-}$  binding, proton transfer through the hydrogen-bonding network to the Mn(III)-bond hydroxide, and electron transfer from the bound  $O_2^{\cdot-}$  to the metal.

As discussed above,  $k_{22}/k_{23}$  will determine the amount of  $O_2^{\cdot-}$  reacting through an outer (reaction 22) versus inner-sphere (reactions 23 and 24) pathway. When reaction (23) is accessed, the product-inhibited complex will be formed and hydrogen peroxide production will be determined by the rate of dissociation of the complex,  $k_{24}$  in reaction (24). This reaction is expected to reflect the rate for protonation off of the  $O_2^{\cdot-}$  in the inhibited-product. Like  $k_{22}$ ,  $k_{24}$  is strongly affected by mutations in the residues involved in the

hydrogen-bonded network. Mutation of Y34 to histidine, glutamine, phenylalanine and valine leads to large variation in  $k_{24}$  (see Table 1). Y34A, Y34N, Y34V, and Y34Q all show a fast protonation off of the bound superoxide and all but Y34V seem to show that loss of peroxide involves two processes, with the detection of a second intermediate species. In these cases, the first process seems to vary with pH. The nature of the second intermediate is still unclear.

Interestingly, for both *D. radiodurans* and *E. coli* MnSOD,  $k_{24}$  is 4 and 2 times slower than in the human enzyme, respectively. Furthermore, Y34F mutation in the *D. radiodurans* enzyme leaves  $k_{24}$  unaltered. This together with the fact that Y34F in the human enzyme decreases  $k_{24}$  to values close to those observed in the prokaryotic enzymes, may reflect small geometric changes due to the point mutation or, instead, slight different mechanisms for protonation off the inhibited-product in the two families of MnSODs[Float1]. In contrast, changes in histidine 30, such as seen in H30N and H30Q, leave the gating between inner-and outer-sphere unaltered but significantly increase the rate of protonation off of the bound  $O_2^{\cdot-}$  in the human enzyme (Table 1).

Two other residues that appear to be involved in product dissociation are E162 and F66, in the human enzyme. All mutations of E162 (see Table 1) and F66 have decreased  $k_{24}$  when compared to the human WT MnSOD. These rates are closer to the one observed for prokaryotic enzymes. Together with the particularity of F66L also having a more *E. coli* gating between inner-and outer-sphere pathways, these results suggest that understanding the differences in the mechanisms of eukaryotic vs. prokaryotic MnSODs lies in understanding some of the effects of the interfaces between the monomeric units on catalysis.

### 5.2. Variation among species

When comparing prokaryotic and eukaryotic MnSOD, some interesting differences in catalysis with possible physiological relevance are evident. Unfortunately, these differences are based on the comparison of a very small number of enzymes, and the analysis of more eukaryotic MnSOD is crucial to probe the true relevance of the different catalytic mechanisms displayed. Although the rate of inhibited-product is higher in human MnSOD, when compared to studied prokaryotic MnSODs (*Bacillus stearothermus* [70]; *Thermus thermophilus* [17]; *E. coli* [69]; *D. radiodurans* [77]) its efficiency at eliminating a higher  $O_2^{\cdot-}$  concentration is lower. This happens, because  $k_{22}/k_{23}$  in human MnSOD leads to saturation of the enzyme at  $O_2^{\cdot-}$ :enzyme ratios not much higher than 1, while in prokaryotic MnSOD, much higher ratios are needed. As an extreme example, the *D. radiodurans* MnSOD starts showing saturation features at ratios close to 40:1 [77]. Apparently, the eukaryotic enzyme delays the prompt release of high hydrogen peroxide fluxes, which can be interpreted as part of a regulation mechanism controlling the cellular concentration of hydrogen peroxide. This is particularly important in human cells, as slight changes in  $H_2O_2$  steady-state concentrations has been proposed to play a part in determining cell fate, such as proliferation or apoptosis [87,88], or in the maintenance of a specific reducing gradient [88], and it is likely that it is equally relevant in other eukaryotic systems. As in eukaryotic systems, in prokaryotes,  $H_2O_2$  also induces the synthesis of new proteins that protect the cells against the effects of oxidative stress damage. Still it is expected that prokaryotes do not need a hydrogen peroxide regulation system as elaborate as eukaryotes, since  $H_2O_2$  can also be eliminate to the cell surrounding environment through membrane diffusion. Thus, it appears that a rapid removal of superoxide in prokaryotes is paramount, regardless of hydrogen peroxide production, while in human cells (and most probably other eukaryotic systems) the rate of peroxide production may be as crucial as the rate of superoxide removal, at least within mitochondria, one of the major sources of ROS in eukaryotic cells.

**Table 1**  
Individual rate constants in the kinetic-mechanism of different MnSODs and their mutants.

MnSOD	$k_{21}$ ( $nM^{-1} s^{-1}$ )	$k_{22}$ ( $nM^{-1} s^{-1}$ )	$k_{23}$ ( $nM^{-1} s^{-1}$ )	$k'_{23}$ ( $s^{-1}$ )	$k_{24}$ ( $s^{-1}$ )
Human <sup>a</sup>	1.5	1.1	1.1	–	120
Y34A <sup>a</sup>	0.25	<0.02	0.38	1600	330
Y34N <sup>a</sup>	0.14	<0.02	0.15	850	200
Y34H <sup>a</sup>	0.07	<0.02	0.04	250	61
Y34V <sup>a</sup>	0.15	<0.02	0.15	–	1000
Y34F <sup>b</sup>	0.55	<0.02	0.46	–	52
H30N <sup>c</sup>	0.21	0.40	0.68	–	480
H30Q <sup>c</sup>	0.57	0.79	0.79	–	200
H30V <sup>c</sup>	~0.005	~0.03	0.16	–	0.7
E162D <sup>d</sup>	0.36	0.13	0.21	–	40
E162A <sup>d</sup>	0.06	0.05	0.09	–	30
F66A <sup>e</sup>	0.6	0.5	0.7	–	82
F66L <sup>e</sup>	0.7	0.8	0.2	–	40
W123F <sup>f</sup>	0.76	<0.02	0.64	–	79
Y166F <sup>d</sup>	0.2	0.2	0.2	–	270
W161A <sup>g</sup>	0.08	<0.01	0.37	–	180
W161F <sup>g</sup>	0.3	<0.01	0.46	–	33
W161V <sup>g</sup>	na	na	0.27	–	265
W161Y <sup>g</sup>	na	na	0.20	–	130
W161H <sup>g</sup>	na	na	0.29	–	136
H30F/Y166F <sup>b</sup>	0.1	0.1	0.1	–	440
Y34F/W123F <sup>f</sup>	0.55	<0.22	0.46	–	52
<i>E. coli</i> <sup>e</sup>	1.1	0.9	0.2	–	60
<i>D. radiodurans</i> <sup>h</sup>	1.2	1.1	0.07	–	30
Y34F <sup>h</sup>	0.9	0.9	0.5	–	30

na, non-available [77].

<sup>a</sup> from [73].

<sup>b</sup> from [93].

<sup>c</sup> from [81].

<sup>d</sup> from [84].

<sup>e</sup> from [85].

<sup>f</sup> from [74].

<sup>g</sup> from [83].

<sup>h</sup> from [77].

A good illustration for this fact comes from the work of Davis et al. [82] where the presence of an enzyme with a higher  $k_{24}$ , and consequently more rapid  $\text{H}_2\text{O}_2$  production, was shown to lead to dramatic *in vivo* effects. The transient overexpression of H30N in human cell lines led to an increase in cell viability in a TNF-mediated apoptosis model, while stable overexpression of this mutated enzyme resulted in a strong anti-proliferative effect upon the transformed cells. While the H30N MnSOD induced cytoprotection was not observed in stable H30N transformed cell lines, suggesting that TNF cytotoxicity is not solely dependent on a  $\text{O}_2^{\cdot-}$  level increase, the authors show that the overexpression of mitochondrial-targeted catalase can rescue H30N MnSOD anti-proliferative phenotype, establishing an important regulation effect for  $\text{H}_2\text{O}_2$  produced during MnSOD catalysis. Furthermore, H30N MnSOD *in vivo* overexpression shows a striking inhibition of tumor growth in an Animal model of tumorigenesis [82], again underlining the importance of MnSOD and particularly MnSOD-derived  $\text{H}_2\text{O}_2$  production in cellular growth control.

The control of MnSOD catalytic features is though accomplished through the fine tuning of a quite unique characteristic of MnSOD mechanism, which is its possibility to eliminate superoxide by two different pathways, a slow protonation off of superoxide (reactions 23 and 24), and a fast protonation off of superoxide (reaction 22). The way this fine tuning is accomplished has been a focus of several studies (see above), but it is still far from being understood. It is important to notice that the crystal structures from different MnSODs show a very high degree of similarity around the active center, while interestingly eukaryotic enzymes are tetramers while prokaryotic are dimers (Fig. 5). This makes the dimer–tetramer interface a promising area to probe. The extensive mutagenesis work done on these enzymes so far suggests that the conditions leading to differences in the mechanisms displayed within this family of proteins is not controlled by a single feature, and that new approaches may be needed to understand MnSOD catalysis nuances. The most interesting overall question as whether this difference in the  $k_{22}/k_{23}$  ratio represents an evolutionary phenomenon without any functional consequence or whether there is actually a functional driver. The evidence given above suggests the latter but more research is definitely needed.

## 6. Nickel superoxide dismutase

The most recently identified superoxide dismutases is nickel superoxide dismutase (NiSOD). This enzyme has been isolated from a number of *Streptomyces* bacteria and from cyanobacteria. The crystal structure has been published by two groups [89,90] and show a hexameric structure with a molecular weight of approximately 80,000 Daltons, where each monomeric unit contains what has been described as a “nickel-hook.” Each nickel is bound by a small peptide chain with binding ligands that consist of two amides, one from the N-terminal and one from the backbone of cysteine 2, two thiolates, one from cysteine 2 and one from cysteine 6, and an imidazole from histidine 3. This is the first SOD in which the binding ligands are anything other than histidines, aspartates and water/hydroxide. The nickel is redox active but the details of the mechanism are still to be unraveled, in large part because of the complexity of making nickel redox active with superoxide.

One significant difference between NiSOD and the other SODs is the apparent lack of ionic strength effect on the catalytic rate constant [91], suggesting there is limited need to generate an electrostatic funneling mechanism. Thus far, preparation of a short chain peptide to mimic the nickel hook region has failed to produce a functional NiSOD mimic although it has produced spectroscopic mimics [92]. The role of the protein is clearly crucial but the details remain to be elucidated.

## Acknowledgements

The authors would like to thank Dr. Célia Romão for valuable assistance with Figs. 5 and 7. I.A.A. was supported by a Post-doctoral fellowship (SFRH/BPD/20581/2004/BH49) from Fundação para a Ciência e Tecnologia, Portugal.

## References

- [1] B.H. Bielski, Fast kinetic studies of dioxygen-derived species and their metal complexes, *Philos. Trans. R. Soc. London* 311 (1985) 473–482.
- [2] D.H. Flint, E. Smyk-Randall, J.F. Tuminello, B. Draczynska-Lusiak, O.R. Brown, The inactivation of dihydroxy-acid dehydratase in *Escherichia coli* treated with hyperbaric oxygen occurs because of the destruction of its Fe-S cluster, but the enzyme remains in the cell in a form that can be reactivated, *J. Biol. Chem.* 268 (1993) 25547–25552.
- [3] D.H. Flint, J.F. Tuminello, M.H. Emptage, The inactivation of Fe-S cluster containing hydro-lyases by superoxide, *J. Biol. Chem.* 268 (1993) 22369–22376.
- [4] F.S. Archibald, I. Fridovich, The scavenging of superoxide radical by manganous complexes: *in vitro*, *Arch. Biochem. Biophys.* 214 (1982) 452–463.
- [5] I. Fridovich, Superoxide radical and superoxide dismutases, *Annu. Rev. biochem.* 64 (1995) 97–112.
- [6] I. Bertini, S. Magnani, M.-S. Viezzoli, Structure and properties of copper–zinc superoxide dismutases. in: S.A.G. (Ed.), *Advances in Inorganic Chemistry*, Academic Press, New York, 1998, pp. 127–250.
- [7] A.R. Reddi, L.T. Jensen, A. Naranuntarat, L. Rosenfeld, E. Leung, R. Shah, V.C. Culotta, The overlapping roles of manganese and Cu/Zn SOD in oxidative stress protection, *Free Rad. Biol. Med.* 46 (2009) 154–162.
- [8] M.J. Daly, E.K. Gaidamakova, V.Y. Matrosova, A. Vasilenko, M. Zhai, A. Venkateswaran, M. Hess, M.V. Omelchenko, H.M. Kostandarithes, K.S. Makarova, L.P. Wackett, J.K. Fredrickson, D. Ghosal, Accumulation of Mn(II) in *Deinococcus radiodurans* facilitates gamma-radiation resistance, *Science (New York, N.Y.)* 306 (2004) 1025–1028.
- [9] F.S. Archibald, I. Fridovich, Manganese and defenses against oxygen toxicity in *Lactobacillus plantarum*, *J. Bacteriol.* 145 (1981) 442–451.
- [10] K. Barnese, E.B. Gralla, D.E. Cabelli, J.S. Valentine, Manganous phosphate acts as a superoxide dismutase, *J. Am. Chem. Soc.* 130 (2008) 4604–4606.
- [11] B.H. Bielski, R.L. Arudi, D.E. Cabelli, W. Bors, Reevaluation of the reactivity of hydroxylamine with  $\text{O}_2^{\cdot-}/\text{HO}_2$ , *Anal. Biochem.* 142 (1984) 207–209.
- [12] G.V. Buxton, Aqueous solutions, in: M.A. Rodgers Farhatziz (Ed.), *Radiation Chemistry*, VCH Publishers Inc, 1987, pp. 321–349.
- [13] H.A. Schwarz, Free radicals generated by radiolysis of aqueous solutions, *J. Chem. Ed.* 58 (1981) 101–105.
- [14] G.V. Buxton, C.L. Greenstock, W.P. Helman, A.B. Ross, Critical review of rate constants for reactions of hydrated electrons, hydrogen atoms and hydroxyl radicals in aqueous solution, *J. Phys. Chem. Ref. Data* 17 (1988) 513–886.
- [15] J.S. Valentine, A.R. Miksztal, D.T. Sawyer, Methods for the study of superoxide chemistry in nonaqueous solutions, *Methods Enzymol.* 105 (1984) 71–81.
- [16] J.A. Fee, C. Bull, Steady-state kinetic studies of superoxide dismutases. Saturative behavior of the copper- and zinc-containing protein, *J. Biol. Chem.* 261 (1986) 13000–13005.
- [17] C. Bull, E.C. Niederboffe, T. Yoshida, J.A. Fee, Kinetic studies of superoxide dismutases: properties of the manganese-containing protein from *Thermus thermophilus*, *J. Am. Chem. Soc.* 113 (1991) 4069–4076.
- [18] M.S. Lah, M.M. Dixon, K.A. Patridge, W.C. Stallings, J.A. Fee, M.L. Ludwig, Structure–function in *Escherichia coli* iron superoxide dismutase: comparisons with the manganese enzyme from *Thermus thermophilus*, *Biochemistry* 34 (1995) 1646–1660.
- [19] J.M. McCord, I. Fridovich, Superoxide dismutase. An enzymic function for erythrocyte (hemocuprein), *J. Biol. Chem.* 244 (1969) 6049–6055.
- [20] M.A. Hough, S.S. Hasnain, Structure of fully reduced bovine copper zinc superoxide dismutase at 1.15 Å, *Structure* 11 (2003) 937–946.
- [21] V.C. Culotta, L.W. Klomp, J. Strain, R.L. Casareno, B. Krems, J.D. Gitlin, The copper chaperone for superoxide dismutase, *J. Biol. Chem.* 272 (1997) 23469–23472.
- [22] P.J. Schmidt, T.D. Rae, R.A. Pufahl, T. Hamma, J. Strain, T.V. O’Halloran, V.C. Culotta, Multiple protein domains contribute to the action of the copper chaperone for superoxide dismutase, *J. Biol. Chem.* 274 (1999) 23719–23725.
- [23] J.M. Leitch, P.J. Yick, C.V. L., The right to choose: Multiple pathways for activating Cu/Zn superoxide dismutases, *Bol Chem.* 284 (2009) 24679–24683.
- [24] A.L. Caruano-Yzermans, T.B. Bartnikas, J.D. Gitlin, Mechanisms of the copper-dependent turnover of the copper chaperone for superoxide dismutase, *J. Biol. Chem.* 281 (2006) 13581–13587.
- [25] D. Klug-Roth, I. Fridovich, J. Rabani, Pulse radiolytic investigations of superoxide catalyzed disproportionation. Mechanism for bovine superoxide dismutase, *J. Am. Chem. Soc.* 95 (1973) 2786–2790.
- [26] G. Rotilio, R.C. Bray, E.M. Fielden, A pulse radiolysis study of superoxide dismutase, *Biochim. Biophys. Acta* 268 (1972) 605–609.
- [27] W.H. Koppenol, Superoxide dismutase and oxygen toxicity, *Bulletin europeen de physiopathologie respiratoire* 17 Suppl. (1981) 85–90.
- [28] A. Cudd, I. Fridovich, Electrostatic interactions in the reaction mechanism of bovine erythrocyte superoxide dismutase, *J. Biol. Chem.* 257 (1982) 11443–11447.
- [29] E.D. Getzoff, J.A. Tainer, P.K. Weiner, P.A. Kollman, J.S. Richardson, D.C. Richardson, Electrostatic recognition between superoxide and copper, zinc superoxide dismutase, *Nature* 306 (1983) 287–290.

- [30] C.L. Fisher, D.E. Cabelli, J.A. Tainer, R.A. Hallelwell, E.D. Getzoff, The role of arginine 143 in the electrostatics and mechanism of Cu,Zn superoxide dismutase: computational and experimental evaluation by mutational analysis, *Proteins* 19 (1994) 24–34.
- [31] E.D. Getzoff, D.E. Cabelli, C.L. Fisher, H.E. Parge, M.S. Viezzoli, L. Banci, R.A. Hallelwell, Faster superoxide dismutase mutants designed by enhancing electrostatic guidance, *Nature* 358 (1992) 347–351.
- [32] L.M. Ellerby, D.E. Cabelli, J.A. Graden, J.S. Valentine, Copper–zinc superoxide dismutase: why not pH-dependent, *J. Am. Chem. Soc.* 118 (1996) 6556–6561.
- [33] R.C. Bray, S.A. Cockle, E.M. Fielden, P.B. Roberts, G. Rotilio, L. Calabrese, Reduction and inactivation of superoxide dismutase by hydrogen peroxide, *Biochem. J.* 139 (1974) 43–48.
- [34] E.K. Hodgson, I. Fridovich, The interaction of bovine erythrocyte superoxide dismutase with hydrogen peroxide: inactivation of the enzyme, *Biochemistry* 14 (1975) 5294–5299.
- [35] T. Kurahashi, A. Miyazaki, S. Suwan, M. Isobe, Extensive investigations on oxidized amino acid residues in H(2)O(2)-treated Cu,Zn-SOD protein with LC-ESI-Q-TOF-MS, MS/MS for the determination of the copper-binding site, *J. Am. Chem. Soc.* 123 (2001) 9268–9278.
- [36] H.J. Fuchs, C.L. Borders Jr, Affinity inactivation of bovine Cu,Zn superoxide dismutase by hydroperoxide anion, HO<sub>2</sub>, *Biochem. Biophys. Res. Commun.* 116 (1983) 1107–1113.
- [37] D.E. Cabelli, D. Allen, B.H. Bielski, J. Holcman, The interaction between Cu(I) superoxide dismutase and hydrogen peroxide, *J. Biol. Chem.* 264 (1989) 9967–9971.
- [38] J.S. Valentine, P.A. Doucette, S. Zittin Potter, Copper-zinc superoxide dismutase and amyotrophic lateral sclerosis, *Annu. Rev. biochem.* 74 (2005) 563–593.
- [39] D.E. Cabelli, Oxidative stress in familial amyotrophic lateral sclerosis, in: L. Packer, J. Fuchs, M. Podda (Eds.), *Redox Genome Interactions in Health and Disease*, Marcel Dekker, Inc., New York, 2003.
- [40] D.R. Rosen, T. Siddique, D. Patterson, D.A. Figlewicz, P. Sapp, A. Hentati, D. Donaldson, J. Goto, J.P. O'Regan, H.X. Deng, et al., Mutations in Cu/Zn superoxide dismutase gene are associated with familial amyotrophic lateral sclerosis, *Nature* 362 (1993) 59–62.
- [41] M.E. Gurney, H. Pu, A.Y. Chiu, M.C. Dal Canto, C.Y. Polchow, D.D. Alexander, J. Caliendo, A. Hentati, Y.W. Kwon, H.X. Deng, et al., Motor neuron degeneration in mice that express a human Cu,Zn superoxide dismutase mutation, *Science* (New York, N.Y.) 264 (1994) 1772–1775.
- [42] M.E. Ripps, G.W. Huntley, P.R. Hof, J.H. Morrison, J.W. Gordon, Transgenic mice expressing an altered murine superoxide dismutase gene provide an animal model of amyotrophic lateral sclerosis, *Proc. Natl. Acad. Sci. U. S. A.* 92 (1995) 689–693.
- [43] T.L. Williamson, D.W. Cleveland, Slowing of axonal transport is a very early event in the toxicity of ALS-linked SOD1 mutants to motor neurons, *Nature Neurosci.* 2 (1999) 50–56.
- [44] J. de Bellerocoe, R.W. Orrell, L. Virgo, Amyotrophic lateral sclerosis: recent advances in understanding disease mechanisms, *J. Neuropathol. Exp. Neurol.* 55 (1996) 747–757.
- [45] L.J. Hayward, J.A. Rodriguez, J.W. Kim, A. Tiwari, J.J. Goto, D.E. Cabelli, J.S. Valentine, R.H. Brown Jr, Decreased metallation and activity in subsets of mutant superoxide dismutases associated with familial amyotrophic lateral sclerosis, *J. Biol. Chem.* 277 (2002) 15923–15931.
- [46] M. Wiedau-Pazos, J.J. Goto, S. Rabizadeh, E.B. Gralla, J.A. Roe, M.K. Lee, J.S. Valentine, D.E. Bredesen, Altered reactivity of superoxide dismutase in familial amyotrophic lateral sclerosis, *Science* (New York, N.Y.) 271 (1996) 515–518.
- [47] M.B. Yim, J.H. Kang, H.S. Yim, H.S. Kwak, P.B. Chock, E.R. Stadtman, A gain-of-function of an amyotrophic lateral sclerosis-associated Cu,Zn-superoxide dismutase mutant: An enhancement of free radical formation due to a decrease in Km for hydrogen peroxide, *Proc. Natl. Acad. Sci. U. S. A.* 93 (1996) 5709–5714.
- [48] J.J. Goto, E.B. Gralla, J.S. Valentine, D.E. Cabelli, Reactions of hydrogen peroxide with familial amyotrophic lateral sclerosis mutant human copper-zinc superoxide dismutases studied by pulse radiolysis, *J. Biol. Chem.* 273 (1998) 30104–30109.
- [49] J.J. Goto, H. Zhu, R.J. Sanchez, A. Nersissian, E.B. Gralla, J.S. Valentine, D.E. Cabelli, Loss of in vitro metal ion binding specificity in mutant copper-zinc superoxide dismutases associated with familial amyotrophic lateral sclerosis, *J. Biol. Chem.* 275 (2000) 1007–1014.
- [50] S.I. Liochev, I. Fridovich, Bicarbonate-enhanced peroxidase activity of Cu,Zn SOD: is the distal oxidant bound or diffusible? *Arch. Biochem. Biophys.* 421 (2004) 255–259.
- [51] J.S. Elam, K. Malek, J.A. Rodriguez, P.A. Doucette, A.B. Taylor, L.J. Hayward, D.E. Cabelli, J.S. Valentine, P.J. Hart, An alternative mechanism of bicarbonate-mediated peroxidation by copper-zinc superoxide dismutase: rates enhanced via proposed enzyme-associated peroxy carbonate intermediate, *J. Biol. Chem.* 278 (2003) 21032–21039.
- [52] D.B. Medinas, G. Cerchiari, D.F. Trindade, O. Augusto, The carbonate radical and related oxidants derived from bicarbonate buffer, *IUBMB life* 59 (2007) 255–262.
- [53] S.I. Liochev, I. Fridovich, CO<sub>2</sub> enhanced peroxidase activity of SOD1: the effects of pH, *Free Rad. Biol. Med.* 36 (2004) 1444–1447.
- [54] M.G. Bonini, S.A. Gabel, K. Rangelova, K. Stadler, E.F. Derose, R.E. London, R.P. Mason, Direct magnetic resonance evidence for peroxy monocarbonate involvement in the Cu,Zn-superoxide dismutase peroxidase catalytic cycle, *J. Biol. Chem.* 284 (2009) 14618–14627.
- [55] S.C. Barber, R.J. Mead, P.J. Shaw, Oxidative stress in ALS: a mechanism of neurodegeneration and a therapeutic target, *Biochim. Biophys. Acta* 1762 (2006) 1051–1067.
- [56] F. Lavelle, M.E. McAdam, E.M. Fielden, P.B. Roberts, A pulse-radiolysis study of the catalytic mechanism of the iron-containing superoxide dismutase from *Photobacterium leiognathi*, *Biochem. J.* 161 (1977) 3–11.
- [57] C. Bull, J.A. Fee, Steady state kinetic studies of superoxide dismutases—properties of the iron-containing protein from *Escherichia coli*, *J. Am. Chem. Soc.* 107 (1985) 3295–3304.
- [58] G. Regelsberger, U. Laaha, D. Dietmann, F. Ruker, A. Canini, M. Grilli-Caiola, P.G. Furtmuller, C. Jakopitsch, G.A. Peschek, C. Obinger, The iron superoxide dismutase from the filamentous cyanobacterium *Nostoc PCC 7120*. Localization, overexpression, and biochemical characterization, *J. Biol. Chem.* 279 (2004) 44384–44393.
- [59] F. Yamakura, K. Suzuki, Inactivation of *Pseudomonas* iron-superoxide dismutase by hydrogen peroxide, *Biochimica et biophysica acta* 874 (1986) 23–29.
- [60] B.B. Keele Jr., J.M. McCord, I. Fridovich, Superoxide dismutase from *Escherichia coli* B. A new manganese-containing enzyme, *J. Biol. Chem.* 245 (1970) 6176–6181.
- [61] C.K. Vance, A.F. Miller, Spectroscopic comparisons of the pH dependencies of Fe-substituted (Mn) superoxide dismutase and Fe-superoxide dismutase, *Biochemistry* 37 (1998) 5518–5527.
- [62] L.E. Grove, T.C. Brunold, Second-sphere tuning of the metal ion reduction potentials in iron and manganese superoxide dismutases, *Comm. Inorg. Chem.* 29 (2008) 134–168.
- [63] E. Luk, M. Yang, L.T. Jensen, Y. Bourbonnais, V.C. Culotta, Manganese activation of superoxide dismutase 2 in the mitochondria of *Saccharomyces cerevisiae*, *J. Biol. Chem.* 280 (2005) 22715–22720.
- [64] E.E. Luk, V.C. Culotta, Manganese superoxide dismutase in *Saccharomyces cerevisiae* acquires its metal co-factor through a pathway involving the Nramp metal transporter, *Smf2p*, *J. Biol. Chem.* 276 (2001) 47556–47562.
- [65] E. Luk, M. Carroll, M. Baker, V.C. Culotta, Manganese activation of superoxide dismutase 2 in *Saccharomyces cerevisiae* requires MTM1, a member of the mitochondrial carrier family, *Proc. Natl. Acad. Sci. U. S. A.* 100 (2003) 10353–10357.
- [66] Z. Su, M.F. Chai, P.L. Lu, R. An, J. Chen, X.C. Wang, AtMTM1, a novel mitochondrial protein, may be involved in activation of the manganese-containing superoxide dismutase in Arabidopsis, *Planta* 226 (2007) 1031–1039.
- [67] M.M. Whittaker, J.W. Whittaker, Conformationally gated metal uptake by apomanganese superoxide dismutase, *Biochemistry* 47 (2008) 11625–11636.
- [68] M.M. Whittaker, K. Mizuno, H.P. Bachinger, J.W. Whittaker, Kinetic analysis of the metal binding mechanism of *Escherichia coli* manganese superoxide dismutase, *Biophys. J.* 90 (2006) 598–607.
- [69] M. Pick, J. Rabani, F. Yost, I. Fridovich, The catalytic mechanism of the manganese-containing superoxide dismutase of *Escherichia coli* studied by pulse radiolysis, *J. Am. Chem. Soc.* 96 (1974) 7329–7333.
- [70] M.E. McAdam, R.A. Fox, F. Lavelle, E.M. Fielden, A pulse-radiolysis study of the manganese-containing superoxide dismutase from *Bacillus stearothermophilus*. A kinetic model for the enzyme action, *The Biochemical journal* 165 (1977) 71–79.
- [71] A.F. Miller, K. Padmakumar, D.L. Sorkin, A. Karapetian, C.K. Vance, Proton-coupled electron transfer in Fe-superoxide dismutase and Mn-superoxide dismutase, *Journal of inorganic biochemistry* 93 (2003) 71–83.
- [72] I.A. Abreu, J.A. Rodriguez, D.E. Cabelli, Theoretical studies of manganese and iron superoxide dismutases: superoxide binding and superoxide oxidation, *The journal of physical chemistry* 109 (2005) 24502–24509.
- [73] J.J. Perry, A.S. Hearn, D.E. Cabelli, H.S. Nick, J.A. Tainer, D.N. Silverman, Contribution of human manganese superoxide dismutase tyrosine 34 to structure and catalysis, *Biochemistry* 48 (2009) 3417–3424.
- [74] W.B. Greenleaf, J.J. Perry, A.S. Hearn, D.E. Cabelli, J.R. Lepock, M.E. Stroupe, J.A. Tainer, H.S. Nick, D.N. Silverman, Role of hydrogen bonding in the active site of human manganese superoxide dismutase, *Biochemistry* 43 (2004) 7038–7045.
- [75] V.J. Leveque, C.K. Vance, H.S. Nick, D.N. Silverman, Redox properties of human manganese superoxide dismutase and active-site mutants, *Biochemistry* 40 (2001) 10586–10591.
- [76] P. Quint, R. Reutzel, R. Mikulski, R. McKenna, D.N. Silverman, Crystal structure of nitrated human manganese superoxide dismutase: mechanism of inactivation, *Free Rad. Biol. Med.* 40 (2006) 453–458.
- [77] I.A. Abreu, A. Hearn, H. An, H.S. Nick, D.N. Silverman, D.E. Cabelli, The kinetic mechanism of manganese-containing superoxide dismutase from *Deinococcus radiodurans*: a specialized enzyme for the elimination of high superoxide concentrations, *Biochemistry* 47 (2008) 2350–2356.
- [78] R.A. Edwards, M.M. Whittaker, J.W. Whittaker, E.N. Baker, G.B. Jameson, Outer sphere mutations perturb metal reactivity in manganese superoxide dismutase, *Biochemistry* 40 (2001) 15–27.
- [79] V.J. Leveque, M.E. Stroupe, J.R. Lepock, D.E. Cabelli, J.A. Tainer, H.S. Nick, D.N. Silverman, Multiple replacements of glutamine 143 in human manganese superoxide dismutase: effects on structure, stability, and catalysis, *Biochemistry* 39 (2000) 7131–7137.
- [80] Y. Hsieh, Y. Guan, C. Tu, P.J. Bratt, A. Angerhofer, J.R. Lepock, M.J. Hickey, J.A. Tainer, H.S. Nick, D.N. Silverman, Probing the active site of human manganese superoxide dismutase: the role of glutamine 143, *Biochemistry* 37 (1998) 4731–4739.
- [81] A.S. Hearn, M.E. Stroupe, D.E. Cabelli, C.A. Ramilo, J.P. Luba, J.A. Tainer, H.S. Nick, D.N. Silverman, Catalytic and structural effects of amino acid substitution at histidine 30 in human manganese superoxide dismutase: insertion of valine C gamma into the substrate access channel, *Biochemistry* 42 (2003) 2781–2789.
- [82] C.A. Davis, A.S. Hearn, B. Fletcher, J. Bickford, J.E. Garcia, V. Leveque, J.A. Melendez, D.N. Silverman, J. Zucali, A. Agarwal, H.S. Nick, Potent anti-tumor effects of an active site mutant of human manganese superoxide dismutase. Evolutionary conservation of product inhibition, *J. Biol. Chem.* 279 (2004) 12769–12776.
- [83] A.S. Hearn, M.E. Stroupe, D.E. Cabelli, J.R. Lepock, J.A. Tainer, H.S. Nick, D.N. Silverman, Kinetic analysis of product inhibition in human manganese superoxide dismutase, *Biochemistry* 40 (2001) 12051–12058.

- [84] P.S. Quint, J.F. Domsic, D.E. Cabelli, R. McKenna, D.N. Silverman, Role of a glutamate bridge spanning the dimeric interface of human manganese superoxide dismutase, *Biochemistry* 47 (2008) 4621–4628.
- [85] J. Zheng, J.F. Domsic, D. Cabelli, R. McKenna, D.N. Silverman, Structural and kinetic study of differences between human and *Escherichia coli* manganese superoxide dismutases, *Biochemistry* 46 (2007) 14830–14837.
- [86] T.A. Jackson, A. Karapetian, A.F. Miller, T.C. Brunold, Probing the geometric and electronic structures of the low-temperature azide adduct and the product-inhibited form of oxidized manganese superoxide dismutase, *Biochemistry* 44 (2005) 1504–1520.
- [87] L. Policastro, B. Molinari, F. Larcher, P. Blanco, O.L. Podhajcer, C.S. Costa, P. Rojas, H. Duran, Imbalance of antioxidant enzymes in tumor cells and inhibition of proliferation and malignant features by scavenging hydrogen peroxide, *Mol. Carcinog.* 39 (2004) 103–113.
- [88] G.R. Buettner, C.F. Ng, M. Wang, V.G. Rodgers, F.Q. Schafer, A new paradigm: manganese superoxide dismutase influences the production of H<sub>2</sub>O<sub>2</sub> in cells and thereby their biological state, *Free Rad. Biol. Med.* 41 (2006) 1338–1350.
- [89] J. Wuerges, J.W. Lee, Y.I. Yim, H.S. Yim, S.O. Kang, K. Djinovic Carugo, Crystal structure of nickel-containing superoxide dismutase reveals another type of active site, *Proc. Natl. Acad. Sci. U. S. A.* 101 (2004) 8569–8574.
- [90] D.P. Barondeau, C.J. Kassmann, C.K. Bruns, J.A. Tainer, E.D. Getzoff, Nickel superoxide dismutase structure and mechanism, *Biochemistry* 43 (2004) 8038–8047.
- [91] S.B. Choudhury, J.W. Lee, G. Davidson, Y.I. Yim, K. Bose, M.L. Sharma, S.O. Kang, D.E. Cabelli, M.J. Maroney, Examination of the nickel site structure and reaction mechanism in *Streptomyces seoulensis* superoxide dismutase, *Biochemistry* 38 (1999) 3744–3752.
- [92] J. Shearer, L.M. Long, A nickel superoxide dismutase maquette that reproduces the spectroscopic and functional properties of the metalloenzyme, *Inorg. Chem.* 45 (2006) 2358–2360.
- [93] A.S. Hearn, L. Fan, J.R. Lepock, J.P. Luba, W.B. Greenleaf, D.E. Cabelli, J.A. Tainer, H.S. Nick, D.N. Silverman, Amino acid substitution at the dimeric interface of human manganese superoxide dismutase, *J. Biol. Chem.* 279 (2004) 5861–5866.
- [94] M. DiDonato, L. Craig, M.E. Huff, M.M. Thayer, R.M. Cardoso, C.J. Kassmann, T.P. Lo, C.K. Bruns, E.T. Powers, J.W. Kelly, E.D. Getzoff, J.A. Tainer, ALS mutants of human superoxide dismutase form fibrous aggregates via framework destabilization, *J. Mol. Biol.* 332 (2003) 601–615.
- [95] R.A. Edwards, H.M. Baker, M.M. Whittaker, J.W. Whittaker, G.B. Jameson, E.N. Baker, Crystal structure of *Escherichia coli* manganese superoxide dismutase at 2.1-angstrom resolution, *J. Biol. Inorg. Chem.* 3 (1998) 161–171.
- [96] W.L. DeLano, The PyMOL Molecular Graphics System DeLano Scientific, San Carlos, CA, USA., 2002.
- [97] G.E. Borgstahl, H.E. Parge, M.J. Hickey, W.F. Beyer Jr., R.A. Hallewell, J.A. Tainer, The structure of human mitochondrial manganese superoxide dismutase reveals a novel tetrameric interface of two 4-helix bundles, *Cell* 71 (1992) 107–118.
- [98] R.J. Dennis, E. Micossi, J. McCarthy, E. Moe, E.J. Gordon, S. Kozielski-Stuhrmann, G.A. Leonard, S. McSweeney, Structure of the manganese superoxide dismutase from *Deinococcus radiodurans* in two crystal forms, *Acta Crystallogr.* 62 (2006) 325–329.
- [99] Y. Guan, M.J. Hickey, G.E. Borgstahl, R.A. Hallewell, J.R. Lepock, D. O'Connor, Y. Hsieh, H.S. Nick, D.N. Silverman, J.A. Tainer, Crystal structure of Y34F mutant human mitochondrial manganese superoxide dismutase and the functional role of tyrosine 34, *Biochemistry* 37 (1998) 4722–4730.